Firing and Sustaining Discharge Characteristics in Alternating Current Microdischarge Cell With Three Electrodes

Hyun Kim and Heung-Sik Tae, *Member, IEEE*

***Abstract*—The firing and sustaining characteristics in an ac microdischarge cell with three electrodes are examined based on varying the distances between the three electrodes. In particular, the breakdown voltage and the sustaining voltage are measured as a parameter of the width of the discharge gap between the three electrodes. It is found that the firing and sustaining conditions vary according to the distance between the three electrodes and the discharge characteristics strongly depend on the voltage applied on the three electrode, especially with a wide discharge gap structure.**

***Index Terms*—Breakdown voltage, discharge gap, microdischarge, sustaining voltage, three electrode, wide discharge gap.**

I. Introduction

THE THREE electrodes in an alternating current (ac) microdischarge cell, for example, the three electrodes in an ac plasma-display panel (ac-PDP), consist of two sustain electrodes and one address electrode [1]–[3]. The two sustain electrodes have a coplanar-type structure and are positioned perpendicular to the address electrode. Through the enormous research in recent years, PDP is already in the process of mass production and taking a large market in flat-panel-display area. Nevertheless, the low luminous efficiency of PDP is still a big problem. Thus, recently, research about improving the luminous efficiency of PDP using the wide discharge gap structure has been performed [4]–[6]. It is well-known that the luminous efficiency of the discharge can be improved when the discharge is produced in the wider discharge gap with a positive column region. However, the breakdown and the sustaining voltages increase in proportion to the length of the discharge gap. In this reason, the wide-gap discharge with a positive column is not easily applicable to the current PDP with microdischarge cells. The previous long-gap discharge characteristics have been determined only by the applied voltage on the sustain electrode. In other words, no voltage was applied to the address electrode during a long gap discharge. However, the application of an ac pulse to the address electrode during a sustaining discharge has an significant influence on the discharge characteristics, especially the long-gap discharge characteristics. Accordingly, the firing and sustaining discharge characteristics relative to the distance between the three electrodes in alternating current microdischarge cell with three electrodes need to be investigated for the possible high efficient wide discharge gap ac-PDP. When the distance between the two sustain electrodes is shorter than that between the sustain and address electrodes, the electric field for accelerating charged particles, such as electrons, is mainly generated in the gap region between the two sustain electrodes [7]. As such, the breakdown and sustaining voltages can be easily determined based on the voltage applied to the sustain electrodes [8]. However, as the distance between the two sustain electrodes becomes wider, the electric field generated between the sustain and address electrodes contributes to strengthening the total electric field, thereby affecting the firing and sustaining conditions of the microdischarge. As a result, the firing and sustaining conditions can not be easily determined by the voltage applied to the sustain electrodes when the distance between the two sustain electrodes is wider than that between the sustain and address electrodes. Accordingly, the current paper examines the firing and sustaining characteristics in an ac microdischarge cell with three electrodes based on varying the distances between the three electrodes. In particular, the breakdown and sustaining voltages are measured as a parameter of the width of the discharge gap among the three electrodes. In addition, the discharge characteristics are investigated relative to variations in the distances between the three electrodes.

Manuscript received August 29, 2003; revised October 25, 2003.

The authors are with School of Electronic and Electical Engineering, Kyungpook National University, Daegu 702-701, Korea (e-mail:hstae@ee.knu.ac.kr).

Digital Object Identifier 10.1109/TPS.2004.827623

II. Experimental Setup

A 7.5-in test panel filled with a gas mixture of Ne–Xe (5%) at a pressure of 500 torr is employed in the current study, and the cell structure of a single pixel is shown in Fig. 1. The width of the sustain electrodes (X or Y) is fixed at 300 μm, while the width of the address electrode (Z) is fixed at 80 μm. The X and Y electrodes are covered with glass based dielectric material with the thickness of 38 μm. The height of the closed type barrier rib is 125 μm. The rib height ("b" in Fig. 1) means the distance between the sustain electrodes (X, Y) and the address electrode (Z), which implies that the distance ("b" in Fig. 1) between (X or Y) and (Z) is fixed at 125 μm. Conversely, the discharge gap ("a" in Fig. 1) between the two sustain electrodes, X and Y is varied from 50 to 400 μm: *i.e.*, 50, 100, 200, and 400 μm for the current experiment. Fig. 2 shows a schematic diagram of the optical and electrical measurement system that is used to determine the luminous efficiency from the test cell utilized in this study. The measurement system consists of a 7.5-in test panel, its driving circuit system, an amperemeter, and a color analyzer. The driving circuit system consists of a pair of driving circuits

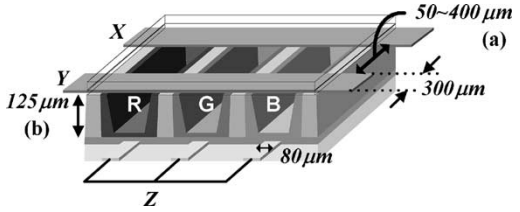

Fig. 1. Three-electrode microdischarge cell structure and specifications employed in this research.

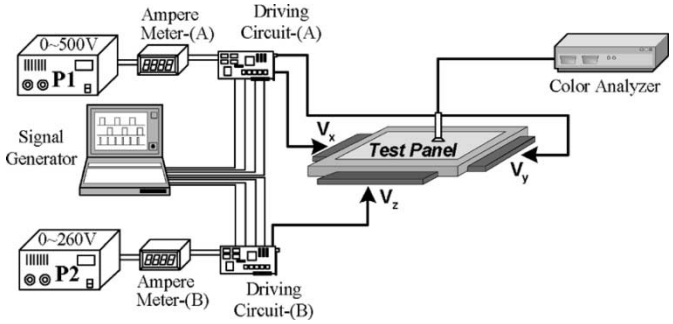

Fig. 2. Schematic diagram of the optical and electrical measurement system.

(A) and (B) and two power supplies P1 and P2. The driving circuit (A) is used to supply the electrical pulses to the sustain electrodes X and Y, whereas the driving circuit (B) is used to supply the electrical pulses to the address electrode Z. The P1 is the power supply for applying the voltage pulses with 0–500 V to the electrodes X and Y. The P2 is the power supply for applying the voltage pulses with 0–260 V to the electrode Z. The sustain circuit (driving circuit (A), power supply P1), and the address circuit (driving circuit (B), power supplies P2) are individually manufactured in order to investigate the effects of voltage pulses V_z, applied to the Z electrode during a sustain-period, on the discharge characteristics. The real current, which flows through the three electrodes during a sustaining discharge, is measured as follows. The sustain current flowing through the sustain electrodes X and Y during a sustain period is measured in the power line between the driving circuit (A) and the power supply P1 by digital amperemeter (A), as shown in Fig. 2. The address current flowing through the electrode Z is also measured in another power line between the driving circuit (B) and the power supply P2 by digital amperemeter (B) as shown in Fig. 2. The additional switch loss during a sustain period is included in power consumption because the currents are measured in front of the driving circuits (A) and (B), as shown in Fig. 2. The luminance of the visible lights emitted from the 7.5-in test panel is measured using a color analyzer (CA-100). The luminous efficiency is defined as follows [9]:

$$\text{Luminous efficiency}\left(\frac{lm}{W}\right) = \frac{\pi \times \text{Luminance}\left(\frac{cd}{m^2}\right) \times \text{Display Area}(m^2)}{\text{Power Consumption}(W)}$$

The power consumption can be the sum of the power consumed through X, Y, and Z electrodes. The power consumption through X and Y electrodes can be calculated from the applied voltage by P1 and the discharge current passing through

TABLE I
FOUR CASES OF CELL STRUCTURES SELECTED ACCORDING TO THE DISTANCE RATIO (a/b) BETWEEN DISCHARGE GAP (a) AND BARRIER RIB HEIGHT (b) EMPLOYED IN THIS RESEARCH

Case	a(㎛)	Comparison	b(㎛)	a/b
Case I	50	<	125	0.4
Case II	100	≈	125	0.8
Case III	200	>	125	1.6
Case IV	400	>>	125	3.2

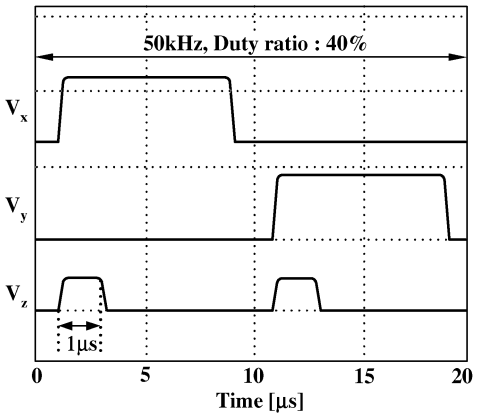

Fig. 3. Voltage waveforms applied to three electrodes.

the amperemeter (A), while the power consumption through Z electrode can be obtained from the applied voltage by P2 and the discharge current measured by the amperemeter (B). Table I shows the four experimental cases based on the distance ratio (a/b) between the discharge gap (a) and the barrier rib height (b). As a matter of a fact, most of the previous researches related to the breakdown and sustaining voltages in the three electrode microdischarge cell are adopting the distance (a) between the two sustain electrodes, X and Y as 60–120μm [10]–[12] and the barrier rib height (b) as 120–150μm [13], [14]. This means that the distance ratio a/b is no more than 1 in the most previous work. In addition, even though there are some reports showing the discharge characteristics of the case where a/b is over 1, no voltage is applied on the address electrode Z in these reports [4]–[6]. Accordingly the experimental case is classified into four cases in order to examine the breakdown and sustaining voltages with the discharge characteristics based on varying the distances between the three electrodes (a/b), while applying the voltage on the address electrode Z. In Table I, case I is when the discharge gap is narrower than the rib height $(a/b < 1)$ and the discharge gap is almost equal to the rib height in Case II $(a/b \approx 1)$. Case III is the case that the discharge gap is wider than the rib height $(a/b > 1)$, whereas case IV is when the discharge gap is much wider than the rib height $(a/b \gg 1)$. The firing and sustaining characteristics of the three-electrode microdischarge are thus discussed based on examining the four experimental cases shown in Table I. Fig. 3 shows the voltage waveforms V_x, V_y, and V_z applied to the sustain electrodes X and Y and address electrode Z, respectively. V_x and V_z with a duty ratio of 40% are applied at a frequency of 50 kHz. V_z is synchronized with each increase in V_x and V_y. Since most of

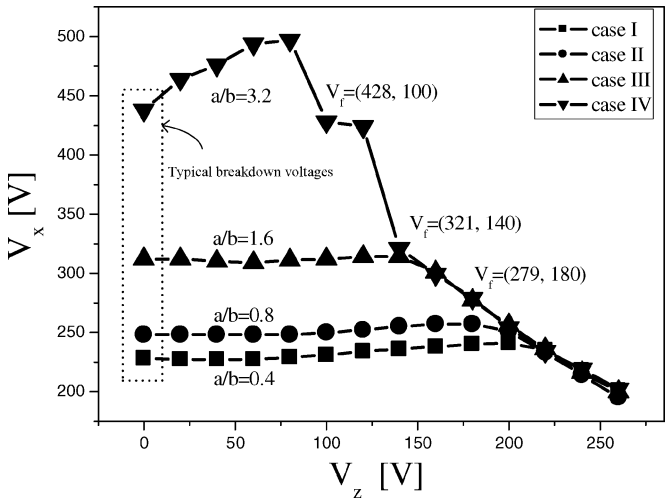

Fig. 4. Breakdown voltage as a function of V_z at various discharge gaps in three-electrode microdischarge cell.

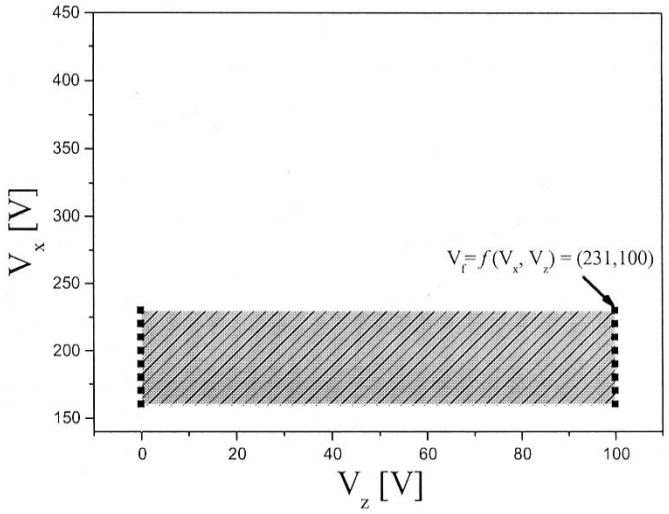

Fig. 5. Sustaining voltage in case of narrow discharge gap structure (50 μm) in case I.

the discharge process in the cell finishes within 1 μs [15], the pulsewidth of V_z is limited to 1 μs.

III. Results and Discussion

Fig. 4 shows the breakdown voltage relative to the applied voltage on the three electrodes for the four experimental cases. The dotted box in Fig. 4 shows the typical breakdown voltages when V_z is grounded: in this case, the breakdown voltage is only determined by V_x or V_y. As shown in Fig. 4, the breakdown voltage increases with an increase in the discharge gap. This phenomenon is well known as Paschen's principle [16]. Fig. 4 also illustrates the breakdown voltages when V_z is applied: in this case, the breakdown voltage is determined by the voltage difference between the three electrodes. Since the amplitude of V_x and V_y is the same in this experiment, the breakdown voltage V_x or V_y is simply represented by V_x. In cases I and II, V_x starts to decrease when V_z is about 200 V. In case III, V_x decreases when V_z is above 140 V, and finally, in case IV, V_x decreases when V_z is above about 80 V. The decrease in the breakdown voltage V_x with the application of V_z indicates that the voltage V_z between the sustain and address electrodes works to ignite the discharge. Meanwhile, the flat region, as shown clearly in cases I, II, and III in Fig. 4, means that the voltage V_z has little effect on the firing in the case of a distance ratio (a/b) below 1.6. Furthermore, the flat region in Fig. 4 shows that the case with a narrower discharge gap has a wider flat region. Meanwhile, the breakdown voltage slightly increases in case IV for $0\ \text{V} < V_z < 100\ \text{V}$, meaning that V_z affects the breakdown voltage. Since the discharge would not be produced between X and Y directly due to the short distance between X and Z, this phenomenon is presumably due to the decrease of the voltage difference by V_z, for example, when $V_x = 450$ V, $V_z = 0$ V, the voltage difference $V_x - V_z = 450$ V, whereas when $V_x = 450$ V, $V_z = 50$ V, the voltage difference $V_x - V_z = 400$ V, therefore, V_x needs to be increased to get more voltage difference between X and Z.

Consequently, as the discharge gap between X and Y becomes wider in comparison with the distance between X (or Y) and Z, the influence of V_z on the firing is intensified. In other words, as the distance between the two sustain electrodes increases, the electric field generated between the sustain and address electrodes contributes to strengthening the total electric field necessary for firing the discharge or possibly forming another discharge mode. As such, the application of V_z has an effect on the firing and sustaining conditions of the microdischarge. In a typical discussion on the breakdown voltage, if the cell structure is fixed, the breakdown voltage only has one value, since the breakdown voltage is determined by V_x or V_y. However, if the effect of V_z on firing is considered, especially in a wide discharge gap structure, there are many breakdown voltages even though the cell structure is fixed. For example, the typical breakdown voltage in case IV is just 430 V, as shown in Fig. 4. However, in the case of applying V_z, the discharge could be fired when $V_x = 428$ V with $V_z = 100$ V, $V_x = 321$ V with $V_z = 140$ V, or $V_x = 279$ V with $V_z = 180$ V. Therefore, the operating voltage V including the breakdown and sustaining voltages, in a three-electrode microdischarge cell can be described as a function of V_x and V_z, *i.e.*, $V = f(V_x, V_z)$, especially in a wide discharge gap structure. The sustaining voltage characteristics of case I are shown in Fig. 5. When the breakdown voltage is taken at $V_f = f(V_x, V_z) = (231, 100)$, the sustaining region expanded with a rectangular shape and the minimum sustaining voltage is $V_s = f(V_x, V_z) = (160, 0)$. When the breakdown voltage is taken at another voltage point, the sustaining region changes, indicating that each breakdown voltage has its own sustaining region. However, when the breakdown voltage is taken from the flat region in Fig. 4, the minimum sustaining voltage does not change, because V_z has almost no effect on firing and sustaining the discharge in this region. Fig. 6 shows the sustaining region in case IV when the discharge is fired at $V_f = f(V_x, V_z) = (428, 100)$ and $V_f = f(V_x, V_z) = (254, 200)$. In the case of $V_f = (428, 100)$, the sustaining region is narrow and located at a high-voltage level. Conversely, in the case of $V_f = (254, 200)$, the sustaining region is wide and located at a low-voltage level. In the case of $V_f = (254, 200)$, the minimum sustaining voltages of

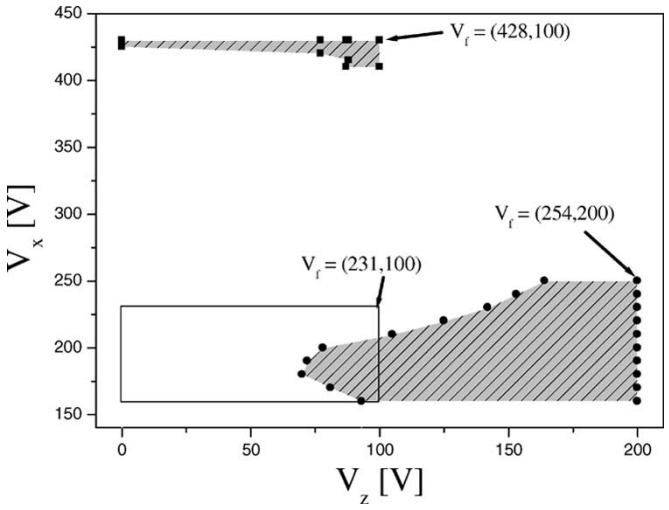

Fig. 6. Sustaining voltage in case of wide discharge gap structure (400 μm) in case IV.

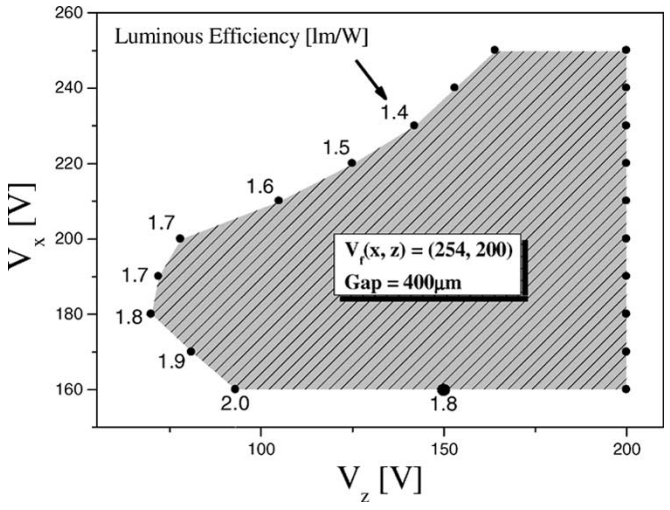

Fig. 7. Luminous efficiency at specific sustaining voltage selected in wide discharge gap structure (400 μm) of case IV.

$V_s = f(\mathrm{V}_x, \mathrm{V}_z)$ are (160, 93), (170, 81), (180, 70), (190, 72), and (200, 78). The upper limits of the sustaining voltages decrease as (254, 164), (240, 153), (230, 142), and (220, 125). When $\mathrm{V}_x = 254$ V, if V_z is controlled below 164 V after firing the discharge at (254, 200), the discharge is not sustained. In addition, when V_z is below 125 V with V_x of 220, the discharge is off. This shows that there exists some possible ratio between V_x and V_z for sustaining the discharge and the firing and sustaining process of the discharge do not depend simply on the electric field intensity. Conversely, high electric field intensity is needed to maintain the discharge when the discharge is fired at $\mathrm{V}_f = (428, 100)$. In addition, after firing the discharge at $\mathrm{V}_f = (428, 100)$ even if the applied voltages are controlled to the sustaining region of the case with $\mathrm{V}_f = (254, 200)$, the discharge is not sustained, meaning that two sustaining regions are completely separated, as shown in Fig. 6. In other words, the experimental result of Fig. 6 indicates that in the wide gap structure, there exist two different discharge modes, and there is no transition between them. This phenomenon can be explained as follows. At $\mathrm{V}_f = (428, 100)$ condition, the voltage distribution between the three electrodes causes a positive charge (i.e., ion) accumulation on the address electrode. On the other hand, at $\mathrm{V}_f = (254, 200)$ condition, the voltage distribution between the three electrodes causes a negative charge (i.e., electron) accumulation on the address electrode. The high electron mobility would contribute to the expansion of the discharge along the address electrode, thus resulting in production of the sustaining discharge at a low voltage level. However, this mechanism should be further studied. On the contrary, the breakdown voltage characteristics shown in Fig. 4 do not clearly show the two discharge modes, however the overlapped decreasing region between case IV and other cases appears to be another discharge mode since this region has almost the same breakdown voltage characteristics in spite of the different X–Y distance. The rectangular solid line in Fig. 6 illustrates the sustaining region of case I shown in Fig. 5 when the discharge gap is narrow. As shown in Fig. 6, an overlapped region exists between the region for $\mathrm{V}_f = (231, 100)$ in case I and that for $\mathrm{V}_f = (254, 200)$ in case IV, indicating that even in the case of a wide discharge gap (400 μm), the discharge can be maintained at a voltage as low as a narrow discharge gap (50 μm) provided that the voltage applied to the three electrodes is properly controlled. Fig. 7 shows the luminous efficiency at the specific sustaining voltages when the discharge is fired at $\mathrm{V}_f = f(\mathrm{V}_x, \mathrm{V}_z) = (254, 200)$ with the wide discharge gap (400 μm) of case IV. When V_x and V_z decrease, the corresponding luminous efficiency increases from 1.4 to 2.0 [lm/W], as the increase in V_x or V_z causes a very high electron temperature [17].

IV. Conclusion

The firing and sustaining characteristics in an ac microdischarge cell with three electrodes are examined based on the voltage applied to the three electrodes with varying discharge gaps. The application of an ac pulse to the address electrode (Z) enables the breakdown and sustaining voltages to be defined according to the voltage applied to the three electrodes, which can be described as a function of V_x and V_z, i.e., $V = f(\mathrm{V}_x, \mathrm{V}_z)$. In addition, the discharge characteristics are found to depend strongly on V_z, especially in a wide discharge gap structure.

References

[1] G. Veronis and U. S. Inan, "Cell geometry designs for efficient plasma display panels," *J. Appl. Phys.*, vol. 92, no. 9, pp. 4897–4905, 2002.

[2] J. H. Seo, W. J. Chung, C. K. Yoon, J. K. Kim, and K. W. Whang, "Two-dimensional modeling of a surface type alternating current plasma display panel cell: Discharge dynamics and address voltage effects," *IEEE Trans. Plasma Sci.*, vol. 29, pp. 824–831, Oct. 2001.

[3] S.-H. Jang, K.-D. Cho, H.-S. Tae, K. C. Choi, and S.-H. Lee, "Improvement of luminance and luminous efficiency using address voltage pulse during sustain-period of AC-PDP," *IEEE Trans. Electron Devices*, vol. 48, pp. 1903–1910, Sept. 2001.

[4] L. F. Weber, " Positive column AC plasma display," U.S. Patent 6 184 848B1, Feb. 6, 2001.

[5] J. Ouyang, T. Callegari, N. Lebarq, B. Caillier, and J.-P. Boeuf, "Plasma display panel cell optimization: Modeling and macro-cell experiments," in *Eurodisplay'02 Dig.*, 2002, pp. 53–56.

[6] T. Callegari, J. Ouyang, N. Lebarq, B. Caillier, and J.-P. Boeuf, "3D modeling of a plasma display panel cell," in *Eurodisplay'02 Dig.*, 2002, pp. 735–738.

[7] H. S. Jeong, B.-J. Shin, and K.-W. Whang, "Two-dimensional multifluid modeling of the He-Xe discharge in and AC plasma display panel," *IEEE Trans. Plasma Sci.*, vol. 27, pp. 171–181, Feb. 1999.

[8] M. F. Gillies and G. Oversluizen, "Influence of the noble gas mixture composition on the performance of a plasma display panel," *J. Appl. Phys.*, vol. 91, pp. 6315–6320, 2002.
[9] C.-H. Park, S.-H. Lee, D.-H. Kim, Y.-K. Kim, and J.-H. Shin, "A study on the new type sustaining electrode showing high luminous efficiency in AC PDPs," *IEEE Trans. Electron Devices*, vol. 48, pp. 2255–2259, Oct. 2001.
[10] G. Oversluizen, M. Kein, S. de Zwart, S. Van Heusden, and T. Dekker, "Improvement of the discharge efficiency in plasma displays," *J. Appl. Phys.*, vol. 91, no. 7, pp. 2403–2408, 2002.
[11] K. C. Choi, B.-J. Baek, and S.-M. Hong, "Plasma display panel employing near ultra violet rays emitted from N2 gas-mixture discharge," in *Proc. 9th Int. Display Workshop*, Hiroshima, Japan, 2002, pp. 801–804.
[12] S.-J. Lee, J.-K. Lee, and H.-J. Hwang, "Improvement of luminance and luminous efficiency by the optimized gas in AC PDP," in *Proc. 9th Int. Display Wrokshop*, Hiroshima, Japan, 2002, pp. 805–808.
[13] Y.-S. Kim, H.-J. Joen, H.-S. Kim, S.-Y. Lee, and S.-K. Hong, "Barrier ribs formed for PDP by rolling of green tape," in *Proc. Soc. Information Display*, 2001, pp. 540–543.
[14] J. K. Kim, J. H. Yang, W. J. Chung, and K. W. Whang, "The addressing characteristics of an alternating current plasma display panel adopting a ramping reset pulse," *IEEE Trans. Electron Devices*, vol. 48, pp. 1556–1563, 2001.
[15] K.-D. Cho, H.-S. Tae, and S.-I. Chien, "Improvement of color temperature using independent control of red, green, blue luminance in AC plasma display panel," *IEEE Trans. Electron Devices*, vol. 50, pp. 359–365, 2003.
[16] S. Uchida, H. Sugawara, Y. Sakai, T. Watanabe, and B.-H. Hong, "Boltzmann equation analysis of electron swarm parameters and related properties of Xe/He and Xe/Ne mixtures used for plasma display panels," *J. Phys. D, Appl. Phys.*, vol. 33, pp. 62–71, 2000.
[17] K. Suzuki, Y. Kawanami, S. Ho, N. Uemura, Y. Yajima, N. Kouchi, and Y. Hatano, "Theoretical formulation of the vacuum ultraviolet production efficiency in a plasma display panel," *J. Appl. Phys.*, vol. 88, pp. 5605–5611, 2000.

Hyun Kim received the B.S. and M.S. degrees in electronic engineering in 1999 and 2002, respectively, from Kyungpook National University, Daegu, Korea, where he is currently working toward Ph.D. degree in electronic engineering.

His current research interests include the microdischarge cell and the driving waveform design of plasma display panels.

Mr. Kim is a member of the Society for Information Display.

Heung-Sik Tae (M'00) received the B.S. degree and the M.S. and Ph.D. degrees in plasma engineering from the Seoul National University, Seoul, Korea, in 1986, 1988, and 1994, respectively.

Since 1995, he has been an Associate Professor with the School of Electronic and Electrical Engineering, Kyungpook National University, Daegu, Korea. His reserch interests include the optical characterization and driving circuit of plasma display panels, the design of millimeter wave guideing structure, and MEMS or thick-film processing for millimeter wave device.

Dr.Tae is a Member of the Society for Information Display.